universe

MDPI

Article

LAMOST J064137.77+045743.8: A Newly Discovered Binary of an A7 Pulsating Subgiant and a Flaring Red Dwarf

Yanhui Chen [1,2,3,*], Chaomi Duan [1,3] and Baokun Sun [1]

[1] Institute of Astrophysics, Chuxiong Normal University, Chuxiong 675000, China; sunbaokun@cxtc.edu.cn (B.S.)
[2] International Centre of Supernovae (ICESUN), Yunnan Key Laboratory, Kunming 650216, China
[3] Faculty of Science, Kunming University of Science and Technology, Kunming 650093, China
* Correspondence: yanhuichen1987@126.com

Abstract

With the progressive release of data from numerous sky surveys, humanity has entered the era of astronomical big data. Multi-wavelength, multi-method research is playing an increasingly crucial role. Binaries account for a substantial fraction of all stellar systems, and research into binaries is of fundamental importance. The low-resolution spectra from Large Sky Area Multi-Object Fiber Spectroscopic Telescope (LAMOST) suggest that LAMOST J064137.77+045743.8 is a binary consisting of an A7-type subgiant star and a cool red dwarf star. LAMOST J064137.77+045743.8 has not yet been recorded in the SIMBAD astronomical database. We conducted a comprehensive analysis of the binary based on multi-wavelength and multi-method research. The spectral analysis suggests that the A7-type subgiant primary star has parameters of $T_{\rm eff} \sim 7500$ K and $\log g \sim 3.9$, and the red dwarf companion star is cool. Additional flux observations in the infrared bands further corroborate the presence of the red dwarf companion, and the near-infrared color index indicates a K4-type red dwarf. Astrometric data from Gaia support the binary speculation with a Renormalized Unit Weight Error metric value of 1.9. The i-band flare detected by the Zwicky Transient Facility (ZTF) photometric observations bolsters the interpretation of the M- or K-type red dwarf companion. Both the radial velocity variations in the Hα lines from LAMOST medium-resolution spectra and the light curves from ZTF support the classification of the A7 subgiant as a pulsating star. No clear evidence of binary eclipses was detected in 1789 days of photometric observations from the ZTF. Future asteroseismology studies will enable us to further probe the internal physics of the A7 subgiant primary star.

Keywords: binary:individual(LAMOST J064137.77+045743.8); flare; pulsation

Check for updates

Academic Editor: Denis Leahy

Received: 22 December 2025
Revised: 21 January 2026
Accepted: 25 January 2026
Published: 27 January 2026

Copyright: © 2026 by the authors. Licensee MDPI, Basel, Switzerland. This article is an open access article distributed under the terms and conditions of the Creative Commons Attribution (CC BY) license.

1. Introduction

The advent of Einstein's mass-energy equation pointed the way for humanity to solve the problem of stellar energy sources. For over a century, despite rapid advancements in various fields of astronomy, the theory of stellar structure and evolution remains one of the most well-established areas in the discipline. The statistical distribution of stars in the Hertzsprung–Russell (H-R) diagram tells us that the vast majority of stars are main-sequence (MS) stars. Stars with an initial mass less than $\sim$2.2 $M_{\odot}$ are classified as low-mass stars. In these stars, the central helium (He) core becomes electron-degenerate before it is ignited. Stars with an initial mass between $\sim$2.2 $M_{\odot}$ and $\sim$9.0 $M_{\odot}$ are classified as intermediate-mass stars. For these stars, the central carbon/oxygen (C/O) core is

electron-degenerate prior to its ignition. Stars with an initial mass greater than $\sim$9.0 $M_{\odot}$ are classified as massive stars. In massive stars, the central C/O core is non-degenerate before ignition. The mass thresholds that separate low-mass, intermediate-mass, and massive stars, based on the degeneracy of their cores at various evolutionary stages, are discussed in standard stellar astrophysics textbooks [1,2]. The vast majority of low- and intermediate-mass stars end their lives as white dwarfs (WDs) [3]. In contrast, massive stars terminate their evolution in a supernova explosion, leaving behind a neutron star or a black hole. Stars constitute the bulk of celestial objects, and stellar physics is the cornerstone of astrophysics, making it a field of paramount importance.

Observational statistics of stars in the solar neighborhood [4,5], as well as simulations of stellar birth rates [6], both indicate that binaries account for a substantial fraction of all stellar systems. Research into binary systems is of fundamental importance. Recent years have witnessed astronomy's entry into a big data era, marked by an abundance of data continuously released from various sky survey telescopes. For the Early Data Release 3 (EDR3) of Gaia [7], Gaia Collaboration presented the Gaia Catalogue of Nearby Stars (GCNS) and reported 16,556 resolved binary candidates [8]. Based on the radial velocity (Rv) data released by the Sloan Digital Sky Survey (SDSS) [9], Pourbaix et al. (2005) derived 675 possible new spectroscopic binary stars and orbits for 8 of them [10]. Thanks to the large field of view and faint limiting magnitude of the Zwicky Transient Facility (ZTF) [11] DR2, Chen et al. (2020) classified 78,602 periodic variables, including $\sim$350,000 eclipsing binaries [12]. Research on binaries is incredibly fascinating.

The Large Sky Area Multi-Object Fiber Spectroscopic Telescope (LAMOST) adopts an innovative active optics technique, giving it both a large aperture (3.6–4.9 m) and a wide field of view (20 square degrees). The distributive parallel-controllable fiber positioning technique enables LAMOST accurately locate 4000 astronomical objects simultaneously [13]. LAMOST focuses on a number of contemporary cutting-edge topics in astrophysics, including the first-generation stars in the Galaxy, the formation and evolution history of galaxies, and the signatures of the distribution of dark matter, and so on, through the northern sky spectral survey [14]. From the pilot survey (24 October 2011 to 17 June 2012) to the twelfth year survey (18 September 2023 to 3 June 2024), LAMOST DR12 low-resolution search (LRS) has released 12,605,485 spectra, including stars, galaxies, quasi-stellar objects, white dwarfs, cataclysmic variable stars, and so on. The LAMOST DR12 medium resolution search (MRS) has released 15,471,948 spectra, including 3,361,604 non-time-domain data and 12,110,344 time-domain data. From 1 October 2024 to 30 June 2025, LAMOST DR13 has released 861,916 LRS spectra and 1,884,766 MRS spectra. The enormous number of celestial spectra provides us with abundant spectral resources for conducting astrophysical research. Qian et al. (2018) reported that by 16 June 2017, LAMOST had observed 3196 EA-type eclipsing binaries, of which 2020 had their atmospheric parameters precisely determined [15].

LAMOST J064137.77+045743.8 is a highly intriguing celestial object that came to the first author's attention during his research on white dwarf spectra. We have confirmed the uniqueness of this target source by inspecting its optical counterpart and cross-matching its positional data from telescopes such as LAMOST and Gaia. Our study reveals that it is a binary system of an A7 pulsating subgiant and a flaring red dwarf, which has not yet been cataloged in the SIMBAD astronomical database. The periodic brightness variations of A7 pulsating subgiants can be used to precisely determine its internal structure, mass, age, and other parameters. Flaring phenomena contribute to understanding stellar magnetic activity in red dwarfs. The dynamical processes in binary systems aid in the study of stellar structure and evolution, angular momentum loss, and potential mass exchange. Such binary systems encompass a wealth of physical principles. In Section 2, we perform a

predictive study for LAMOST J064137.77+045743.8 based on LRS and MRS spectra released by LAMOST. A supplementary verification for LAMOST J064137.77+045743.8 is carried out in Section 3 based on other spectroscopic surveys and imaging surveys. In Section 4, we derive solid evidence of the companion star for LAMOST J064137.77+045743.8 based on data released by the ZTF telescope. At last, we give a discussion and conclusions in Section 5.

2. LAMOST LRS/MRS Spectral Analysis of LAMOST J064137.77+045743.8

For the LAMOST LRS spectra, the wavelength coverage is 3700–9000 Å, including 3700–5900 Å for the blue channel and 5700–9000 Å for the red channel [13]. The LAMOST LRS spectra have a resolution of 1800 [16,17] at the 5500 Å. For the LAMOST MRS spectra, the wavelength coverage is 4950–5350 Å for the blue cameras and 6300–6800 Å for the red cameras, and the resolution is ∼7500 [18].

For the LAMOST LRS spectra, LAMOST J064137.77+045743.8 was observed six times on 18 February 2012, 11 November 2023, 16 November 2023, 17 November 2023, 29 December 2024, and 1 January 2025, with identified spectral types of A5, WD, A7, F0, A7, and A7, respectively, as shown in Table 1. LAMOST releases a vast number of celestial spectra each year from 2011, and the spectral classifications as well as stellar parameters are all derived from the LAMOST stellar parameter pipeline (LASP) [19,20]. For the second spectrum, the signal-to-noise ratio (SNR) is 0.0 for the r, i, and z bands, respectively. The second spectrum could be easily mistaken for a WD; however, the other spectra contain an overabundance of metal lines, as shown in Figure 1 and Table 2. From the [Fe/H] value in Table 1, it can be seen that LAMOST J064137.77+045743.8 is only slightly more metal-poor than the Sun [21]. The four most recent spectra are so similar that they can be brought into close agreement by a simple multiplicative scaling factor. Based on the four recently observed spectra from LAMOST, the derived effective temperature and gravitational acceleration are $T_{\rm eff} \sim 7500$ K and $\log g \sim 3.9$, as shown in Table 1. The relatively weak and narrow absorption lines of Fe II and the Ca II K also indicate that the primary component of the spectrum is contributed by an A7 subgiant star. However, the Ca I line, Na I line, and Fe I line suggest the possible existence of a low-$T_{\rm eff}$ companion star. The Ca II triplet indicates that the companion star is truly a low-$T_{\rm eff}$ star [22]. Based on the LAMOST LRS spectra, LAMOST J064137.77+045743.8 is not a WD but most likely a combined system of an A7-type subgiant star and an M or K-type red dwarf star. Given that all other spectral lines are narrow absorptions, the sole broad emission feature at 6000 Å is likely to be an instrumental or reduction artefact, as this wavelength corresponds to the calibration overlap region between the blue and red arms in LAMOST LRS spectra [23,24].

Table 1. Six observations of LAMOST LRS spectra, indcluding MJD, SNR, and atmospheric parameters.

MJD (Median UTC)	SNR of u, g, r, i, z	Class	$T_{\rm eff}$ [K]	$\log g$	[Fe/H]
55,975.58487	0.66, 8.69, 21.61, 27.60, 20.82	A5	7740.00 ± 79.96	4.097 ± 0.134	−0.250 ± 0.088
60,259.76028	0.44, 2.57, 0.00, 0.00, 0.00	WD	11,567.36 ± 660.63	8.172 ± 0.242	
60,264.70400	25.55, 121.51, 176.69, 213.39, 144.37	A7	7519.43 ± 25.08	3.931 ± 0.034	−0.104 ± 0.019
60,265.72347	42.88, 190.10, 279.75, 337.59, 242.10	F0	7527.08 ± 17.36	3.865 ± 0.022	−0.070 ± 0.011
60,673.58471	42.93, 174.21, 241.35, 303.25, 234.48	A7	7570.27 ± 18.41	3.931 ± 0.024	−0.072 ± 0.013
60,676.58239	44.30, 181.44, 251.35, 319.66, 253.35	A7	7555.08 ± 18.15	3.871 ± 0.023	−0.055 ± 0.012

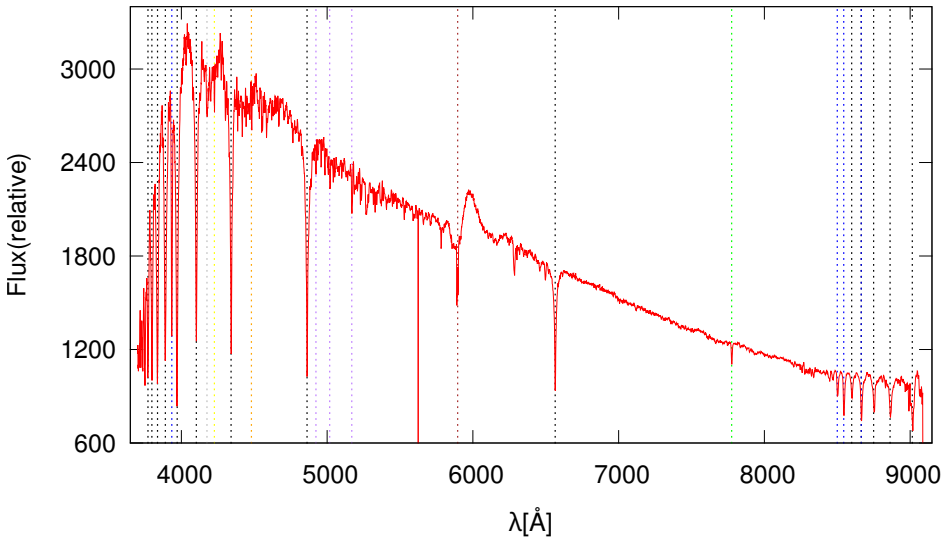

Figure 1. LAMOST DR13 LRS spectrum for LAMOST J064137.77+045743.8 observed in 1 January 2025. The different colored lines represent different absorption lines, as shown in Table 2.

Table 2. Wavelength of absorption lines in angstrom identified in Figure 1.

Absorption Lines	Wavelength [Å]	Color
H9	3771	black
H8	3798	black
Hη	3836.47	black
Hζ	3890.15	black
Hϵ	3971.19	black
Hδ	4102.89	black
Hγ	4341.68	black
Hβ	4862.68	black
Hα	6564.61	black
Paschen (n = 14→n = 3)	8598	black
Paschen (n = 13→n = 3)	8665	black
Paschen (n = 12→n = 3)	8750	black
Paschen (n = 11→n = 3)	8863	black
Paschen (n = 10→n = 3)	9015	black
Fe II	4924	purple
Fe II	5018	purple
Fe II	5169	purple
Mg II	4481	orange
Ca II K	3934.78	blue
Ca II triplet	8500.35, 8544.44, 8664.52	blue
Fe I	4176	grey
Ca I	4227.92	yellow
Na I	5896	brown
O I	7775	green

For the LAMOST DR13 MRS spectra, the recent observational data, LAMOST J064137.77+045743.8 was observed over three days: 7 February, 16 February, and 6 March, 2025. For each day, there are three spectroscopic observations taken at 22 min intervals or longer, with each spectrum covering both the B-band (roughly from 4938 Å to 5380 Å) and R-band (roughly from 6263 Å to 6843 Å). The LAMOST DR13 MRS spectra also support the parameter values of $T_{\rm eff} \sim 7500$ K (7508.13 $\pm$ 18.16 and 7695.40 $\pm$ 23.91) and $\log g \sim 3.9$ (3.970 $\pm$ 0.020 and 3.845 $\pm$ 0.029) for the primary star. In Figure 2, we show the B-band and R-band spectra with MJD = 60,722.56806. The Hα absorption line (black) and the

possible Fe II (purple) and Mg I lines (green) are marked as vertical dashed lines. We obtained the Rvs of nine R-band spectra by fitting the Hα absorption line with a Gaussian function, as shown in Table 3. The wavelength error at the center of the Hα absorption line is on the order of 0.003%. We have also used the Gaussian fitting method to study the value of Rv of a cataclysmic variable star, IU Leo [25]. The Gaussian fitting method for the Hα absorption line was also applied to the six LRS spectra, as shown in Table 3. The maximum Rv is 60.74 km/s and the minimum Rv is 17.81 km/s. With an interval of 22 min, the maximum difference in Rv can reach 25.12 km/s (the last two spectra of MRS). Unlike cataclysmic variables, the variations in the spectroscopic Rv of LAMOST J064137.77+045743.8 should originate from the pulsations of the A7-type subgiant star. This is because binary systems with orbital periods of a few dozen minutes are dynamically unstable or exhibit intense mass transfer that generates emission lines. No emission lines were detected in either LAMOST LRS spectra or LAMOST MRS spectra. In the last column of Table 3, we show the results of Gaussian fitting to the possible diffuse interstellar band (DIB) [26] indicated by the blue arrow in Figure 2. For the MRS spectra, a detailed study of DIBs is challenging. However, the DIB is clearly detected in five MRS spectra, as shown in Table 3. The inconsistent variation trends between the DIB wavelength and the Hα line wavelength in Table 3 support our identification of the DIB.

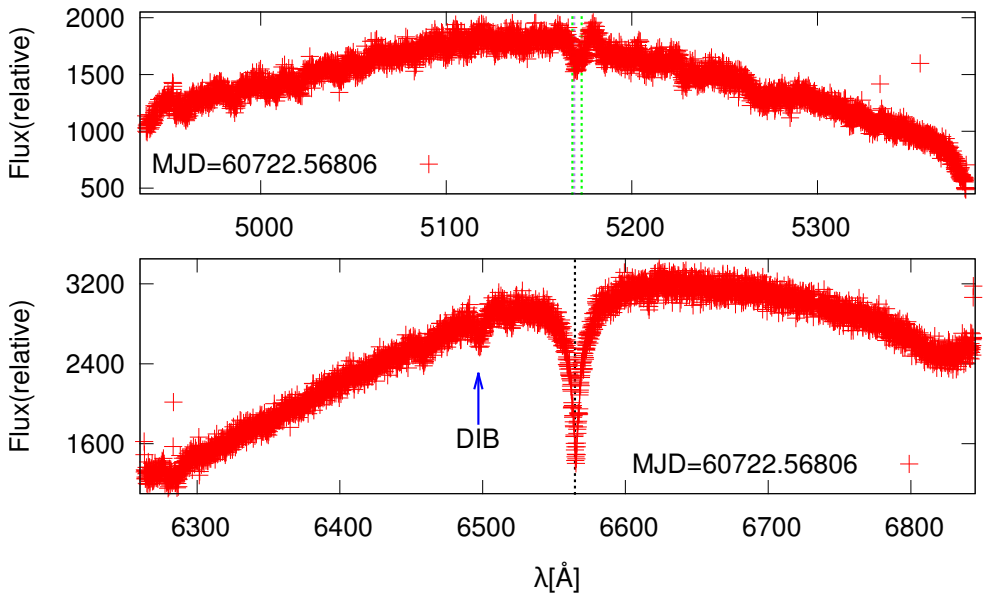

Figure 2. LAMOST DR13 MRS spectra for LAMOST J064137.77+045743.8 observed in 16 February 2025. The observation median UTC time is MJD = 60,722.56806.

Table 3. Rv values of 9 LAMOST MRS R-band spectra and 5 LAMOST LRS spectra.

	MJD (Median UTC)	Wavelength of Hα [Å]	Rv [km/s]	DIB [Å]
MRS	60,713.52153	6565.38 ± 0.21	35.16	
	60,713.56389	6565.58 ± 0.20	44.30	
	60,713.57986	6565.94 ± 0.21	60.74	
	60,722.51181	6565.21 ± 0.15	27.40	6495.31 ± 0.80
	60,722.55278	6565.20 ± 0.20	26.94	6496.00 ± 0.99
	60,722.56806	6565.20 ± 0.15	26.94	6495.83 ± 0.74
	60,740.44444	6565.18 ± 0.21	26.03	6496.60 ± 1.01
	60,740.52083	6565.00 ± 0.17	17.81	6496.60 ± 0.66
	60,740.53611	6565.55 ± 0.27	42.93	

Table 3. *Cont.*

	MJD (Median UTC)	Wavelength of Hα [Å]	Rv [km/s]	DIB [Å]
LRS	55,975.58487	6565.79 ± 0.40	53.89	
	60,259.76028			
	60,264.70400	6565.54 ± 0.26	42.47	
	60,265.72347	6565.54 ± 0.26	42.47	
	60,673.58471	6565.71 ± 0.28	50.24	
	60,676.58239	6565.83 ± 0.28	55.72	

3. Supplementary Analysis: Gaia, SkyMapper, 2MASS, and WISE Data

Multi-wavelength studies are essential for a more comprehensive understanding of the target celestial object. LAMOST J064137.77+045743.8 was not observed by SDSS, but was observed by Gaia, SkyMapper telescope [27], Two Micron All Sky Survey (2MASS) [28], and Wide-field Infrared Survey Explorer (WISE) [29]. In Table 4, we show the apparent magnitude of LAMOST J064137.77+045743.8 in the uvgriz, JHKs, and w1w2w3w4 bands, respectively. The center wavelengths of uvgriz, JHKs, and w1w2w3w4 are from references [27], respectively. The apparent magnitude in the near-infrared band indicates strong radiation in that band, which supports the speculation that the companion star is a low-$T_{\rm eff}$ star. In addition, we calculate the color index among near-infrared bands. The color indices in the optical band should be dominated by the A7 star, while those in the near-infrared band should be dominated by the cool companion star. Compared with the color indices of stars with known spectral types [30], we find that the cool companion star is likely to be of spectral type K4. Due to inconsistencies in the zero-magnitude flux calibrations across the optical, near-infrared, and mid-infrared bands, a combined graphical representation of the data in Table 4 is not presented, as it would not permit a physically meaningful comparison.

In Figure 3, we show the spectral data from LAMOST and Gaia XP (no Rvs Spectrum) together with flux data from SkyMapper, 2MASS, and WISE for LAMOST J064137.77+045743.8. It is important to note that the flux in LAMOST's LRS spectra is relative. The numerical flux values themselves carry no physical meaning, whereas the overall flux profile and relative relationships do hold physical significance. During comparative studies, the relative flux of LAMOST's LRS spectra can be scaled up or down by a factor. The spectrum from LAMOST in 2025 (divided by a factor of 13) is consistent with the flux data (directly from the CDS Portal) observed by the SkyMapper telescope. However, it is inconsistent with the Gaia XP spectrum. It is quite interesting that the spectrum from LAMOST in 2012 (divided by a factor of 2.82) is consistent with the XP spectrum from Gaia. The comparative analysis is performed by manually adjusting the scaling parameters on the LAMOST LRS spectra and relying on visual inspection. The degree of agreement in the spectral profiles is sufficient to draw a reliable conclusion. The flux plot in the lower panel of Figure 3 also demonstrates the deviation from a single blackbody spectrum. The spectra in the upper panel of Figure 3 are likely significantly influenced by the companion star. In the Gaia archive website (https://gea.esac.esa.int/archive/ (accessed on 27 September 2025)), LAMOST J064137.77+045743.8 was fitted by a binary of $T_{\rm eff1} \sim 6750$ K, $\log g_1 \sim 4.55$ and $T_{\rm eff2} \sim 5450$ K, $\log g_2 \sim 3.95$. This was obtained from spectral fitting when the Gaia XP spectrum was significantly influenced by the companion star. We examined the Renormalized Unit Weight Error metric (RUWE) [31] value and found it to be 1.9. It is significantly greater than the threshold of 1.2 [32], which, from an astrometric perspective, indicates the presence of a binary star system.

Table 4. Apparent magnitude for LAMOST J064137.77+045743.8. The values of uvgriz, JHK, and w1w2w3w4 are released by SkyMapper, 2MASS, and WISE, respectively. Some color indexes are calculated for LAMOST J064137.77+045743.8.

filter	u	v	g	r	i	z	J	H	Ks	w1	w2	w3	w4
λ (nm)	355.0	387.0	497.0	604.0	771.0	909.0	1250	1650	2160	3400	4600	12,000	22,000
mag	15.312	14.441	13.394	13.085	12.884	12.736	11.818	11.544	11.451	11.339	11.347	12.286	9.121
err	0.043	0.022	0.012	0.013	0.011	0.016	0.021	0.020	0.019	0.012	0.009	0.412	
color index						i-z	z-J	J-H	H-Ks				
mag						0.148	0.918	0.274	0.093				

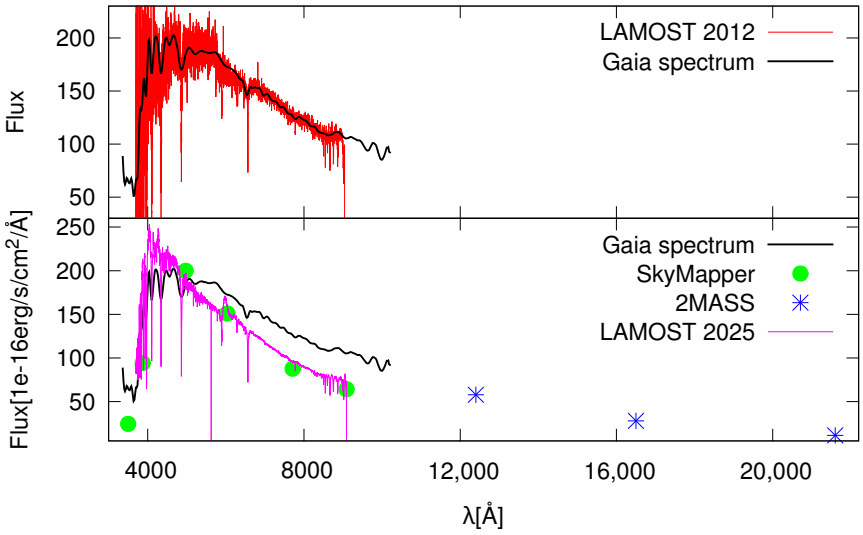

Figure 3. Spectral data from LAMOST and Gaia together with flux data from SkyMapper and 2MASS.

4. Supporting Evidence for the Companion Star from ZTF Data

The Barbara A. Mikulski Archive for Space Telescopes (MAST) [33] hosts data from numerous telescope missions and provides user-friendly access. We identified the target star by directly cross-matching LAMOST's DA-type WD data with MAST's archive data (CLT catalog). Applying the criteria of $T_{\rm eff}$ between 10,600 and 12,600 K and $\log g$ between 7.95 and 8.35 on the LAMOST DR12 LRS Spectra official website, we initially selected 138 candidate spectra of pulsating DA WDs. Upon cross-matching the uploaded data file with the TESS Candidate Target List (CTL) v8.01 on the MAST portal, we successfully identified our target source. Time-domain data are essential for confirming binary systems. Unfortunately, LAMOST J064137.77+045743.8 was not observed by the Kepler mission [34] or the Transiting Exoplanet Survey Satellite (TESS) [35] in the MAST archive. In MAST archive, the stellar parameters of LAMOST J064137.77+045743.8 are $T_{\rm eff}$ = 7657.52 $\pm$ 211.28 K, $\log g$ = 3.73 $\pm$ 0.11, radius = 3.01 $\pm$ 0.24 $R_{\odot}$, mass = 1.79 $\pm$ 0.29 $M_{\odot}$, luminosity = 28.10 $\pm$ 3.65 $L_{\odot}$, and distance = 1848.24 $\pm$ 85.80 pc. These parameters are from the TESS CTL v8.01 data. They are self-consistent and support the classification of the primary star as an A7-type subgiant star.

Open-source astronomical big data is an invaluable asset for all humanity: we have been delighted to have found the light curve for LAMOST J064137.77+045743.8 on the ZTF website. Using a search radius of 1 arcsecond, after entering the coordinates on the ZTF official website, the maximum separation in the existing observational data is only 0.136 arcseconds. Such a small angular separation leads us to consider it as the same source. Moreover, visual inspection of the images confirms that the observations are targeted at the same object. The observations are from 27 March 2018 to 18 February 2023, covering 1789 days, as shown in Figure 4. The ZTF telescope employs a filter system comprising the

g, r, and i bands [36] for transient detection. There are 289, 366, and 27 data points for g, r, and i bands in the lower panel of Figure 4 for LAMOST J064137.77+045743.8. In the middle panel of Figure 4, we can see a brightness variation of approximately 0.06 magnitudes in the g-band, which is consistent with the variation amplitude of δ Sct variables. The same holds for the r-band variation during quiescent periods. In the r-band data, we detected an intermittent flare event. The brightness increased by 0.5 magnitudes, lasting for approximately 100 min, as shown in the upper panel of Figure 4. The ZTF achieves a per-image astrometric precision of approximately 45–85 milliarcseconds relative to the Gaia DR1 [37]. The High Energy Astrophysics Science Archive Research Center (HEASARC) at NASA/GSFC provides public online access to a comprehensive archive of data from major X-ray and gamma-ray astronomy missions [38]. The angular separation to the nearest high-energy burst recorded in HEASARC for this source direction is also greater than 1 degree. Therefore, we have reason to believe that the burst in Figure 4 originated from a flare of the companion of LAMOST J064137.77+045743.8. The detected flare event provides strong evidence that the companion star is likely an M- or K-type red dwarf, as such flares are caused by magnetic reconnection processes in the star's strong magnetic fields, which are generated within its convective zone. Stellar flares are remarkably prevalent. Davenport (2016) reported 4041 flaring stars in Kepler data [39], while Günther et al. (2020) identified 1228 flaring stars in TESS data, of which 673 are M dwarfs [40]. Flares that increase in brightness by about 0.5 magnitudes in a few minutes are observed, including those documented in the TESS flare statistics [41] and shown in Figure 4.

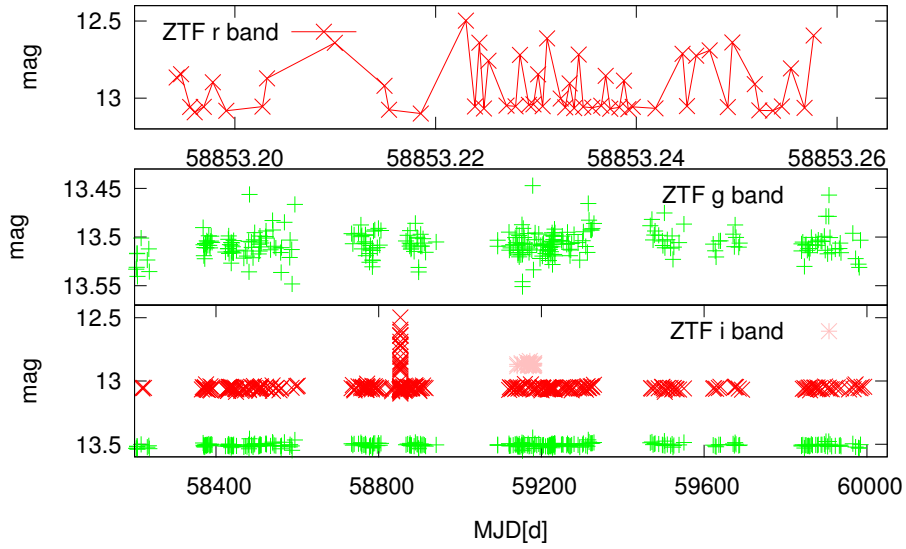

Figure 4. Light curve of g, r, and i bands for LAMOST J064137.77+045743.8 from ZTF.

Based on the light curve, five periods of 71.21, 196.4, 29.01, 6.016, and 27.33 days were derived by a pipeline ztfperiodic [42] on the ZTF website, with corresponding SNRs of 10.09, 9.503, 6.01, 5.749, and 5.716, respectively. No evidence of eclipses was found in over 1789 days of photometric observations, as shown in Figure 4. This non-detection implies several possibilities: First, the binary orbital period could be much longer than our observational baseline of 1789 days. Alternatively, the system could possess a low orbital inclination, placing its orbital plane nearly face-on to our line of sight, which geometrically prevents eclipses from occurring. Finally, even if the inclination is high, the eclipses could be extremely shallow—due to factors such as a large difference in stellar sizes or a high orbital eccentricity—making them undetectable within the precision of our current data. In the Gaia DR3 data, LAMOST J064137.77+045743.8 is located 1848 pc away, making it

extremely challenging to resolve into two point sources even for binary systems with very long orbital periods.

The pulsation periods of δ Sct variables are generally on the order of several hours, which is comparable in magnitude to the time intervals of the MRS spectra in Table 3. Shorter periods could potentially be interference from sub-flares. Periods of several days or tens of days might correspond to the rotation period of a companion star. Rapidly rotating stars can generally produce starspots and modulate their brightness through rotation [39]. Periods of tens or hundreds of days could be related to the orbital period of a binary system (non-eclipsing). Periods of years may be the magnetic activity cycle of a companion. These are only preliminary and qualitative estimates; the specific physical origins of each period require further in-depth study. The phase-folding method did not reveal any clear single periodic signal. Future work may involve a more detailed investigation of periodic signals by analyzing data in different bands and time segments.

5. A Discussion and Conclusions

In recent years, with the continuous release and public availability of large amounts of survey data, astronomical research has entered the era of big data. Multi-wavelength and multi-method studies have proven to be crucial in uncovering the true nature of research targets. In this paper, we report on the serendipitous discovery of the variability of LAMOST J064137.77+045743.8 while cross-matching data from the LAMOST data release with the MAST archive in search of pulsating WDs. It has not yet been cataloged in the SIMBAD astronomical database. We have conducted studies on LAMOST J064137.77+045743.8 using multi-wavelength, multi-method approaches including spectroscopy, astrometry, and photometry.

Among the five valid LRS spectra released by LAMOST, four (three A7-type and one F0-type) match the flux points measured by SkyMapper, while one (A5-type) aligns with the Gaia XP spectrum. Through detailed identification of the absorption lines in the four spectra, we found that in addition to the typical absorption lines of an A7-type star, there are also faint but distinct metal lines characteristic of low-$T_{\rm eff}$ stars, such as Ca I, Na I, Fe I, and the Ca II triplet lines, as shown in Figure 1 and Table 2. Based on the effective temperature ($T_{\rm eff} \sim 7500$ K) and surface gravity ($\log g \sim 3.9$) values [21] derived from the spectroscopic data, along with detailed analysis of specific absorption lines, it is inferred that LAMOST J064137.77+045743.8 is likely a binary system composed of an A7-type subgiant and an M- or K-type red dwarf star. The flux measurements in the JHKs bands from the 2MASS release and the W1, W2, W3, W4 bands from the WISE release also indicate the presence of a low-$T_{\rm eff}$ star. The color index values in the near-infrared band in Table 4 indicate that the spectral type of the cool companion is likely K4 [30].

The RUWE parameter of Gaia for LAMOST J064137.77+045743.8 is 1.9, which indicates the presence of a binary star system [32] from the astrometric perspective. The first spectrum for LAMOST J064137.77+045743.8 released by LAMOST is an A5-type star, consistent with the Gaia XP spectrum. We now know that this should be caused by the magnetic activity of the red dwarf companion star. Multi-wavelength and multi-method studies yield more accurate and comprehensive binary star information than relying solely on Gaia data.

We are truly grateful for open-source astronomical big data. The ZTF telescope has conducted 289, 366, and 27 valid observations in the g, r, and i bands, respectively, for LAMOST J064137.77+045743.8, spanning a time period of 1789 days. In the r-band data, an intermittent stellar flare event with an apparent magnitude variation of 0.5 magnitudes and a duration of approximately 100 min was detected, as shown in the upper panel of Figure 4. The stellar flare event provides strong evidence that the companion star is likely an M- or K-type red dwarf. Therefore, LAMOST J064137.77+045743.8 is a binary with

an A7-type subgiant primary star and an M- or K-type flaring red dwarf companion star. The absence of detectable eclipses implies that the system either has an orbital period longer than our observational baseline, a low orbital inclination (geometrically preventing eclipses), or a high inclination with undetectable shallow eclipses due to the system's physical parameters.

The radial velocity variations derived from the Hα absorption lines in the LAMOST MRS spectra originate from pulsations of the A7-type subgiant star for LAMOST J064137.77+045743.8. The amplitudes of the light curves in the ZTF g and r bands are also consistent with the variation amplitudes of δ Sct variables. Jia et al. (2024) reported a largest catalog (2254) of multimode δ Sct variables in the northern sky using the ZTF DR20 [43]. The asteroseismology of the δ Sct variables is particularly fascinating, as it can even probe the size of the helium core in the stellar center [44]. In the future, we plan to study the periodic signals involving a band-by-band and epoch-separated analysis in the light curves and conduct asteroseismology studies on this A7-type subgiant primary star to probe its internal physics. Pulsating binary systems are both interesting and important, as they encompass a wealth of physical laws.

Author Contributions: Data curation, C.D.; formal analysis, Y.C.; methodology, B.S.; project administration, Y.C.; software, C.D.; supervision, Y.C.; writing—original draft, Y.C. All authors have read and agreed to the published version of the manuscript.

Funding: Guoshoujing Telescope (the Large Sky Area Multi-Object Fiber Spectroscopic Telescope LAMOST) is a National Major Scientific Project built by the Chinese Academy of Sciences. Funding for the project has been provided by the National Development and Reform Commission. LAMOST is operated and managed by the National Astronomical Observatories, Chinese Academy of Sciences. This work is supported by the International Centre of Supernovae, Yunnan Key Laboratory (No. 202302AN36000101) and the Yunnan Provincial Department of Education Science Research Fund Project (No. 2024J0964).

Data Availability Statement: The original contributions presented in this study are included in the article. Further inquiries can be directed to the corresponding author.

Conflicts of Interest: The authors declare no conflicts of interest.

References

1. Prialnik, D. *An Introduction to the Theory of Stellar Structure and Evolution*; Cambridge University Press: Cambridge, UK, 2009.
2. Carroll, B.W.; Ostlie, D.A. *An Introduction to Modern Astrophysics*, 2nd ed.; Cambridge University Press: Cambridge, UK, 2017.
3. Winget, D.E.; Kepler, S.O. Pulsating White Dwarf Stars and Precision Asteroseismology. *Ann. Rev. Astron. Astrophys.* **2008**, *46*, 157–199. [CrossRef]
4. Duquennoy, A.; Mayor, M. Multiplicity among solar-type stars in the solar neighbourhood II. Distribution of the orbital elements in an unbiased sample. *Astron. Astrophys.* **1991**, *248*, 485–524.
5. Raghavan, D.; McAlister, H.A.; Henry, T.J.; Latham, D.W.; Marcy, G.W.; Mason, B.D.; Gies, D.R.; White, R.J.; ten Brummelaar, T.A. A survey of stellar families: Multiplicity of solar-type stars. *Astrophys. J. Suppl. Ser.* **2010**, *190*, 1–42. [CrossRef]
6. Machida, M.N.; Matsumoto, T.; Hanawa, T.; Tomisaka, K. Collapse and fragmentation of rotating magnetized clouds-II. Binary formation and fragmentation of first cores. *Mon. Not. R. Astron. Soc.* **2005**, *362*, 382–402. [CrossRef]
7. Gaia Collaboration. The Gaia mission. *Astron. Astrophys.* **2016**, *595*, A1. [CrossRef]
8. Gaia Collaboration. Gaia Early Data Release 3 The gaia Catalogue of Nearby Stars. *Astron. Astrophys.* **2021**, *649*, A6. [CrossRef]
9. York, D.G.; Adelman, J.; Anderson, J.E.; Anderson, S.F.; Annis, J.; Bahcall, N.A.; Bakken, J.A.; Barkhouser, R.; Bastian, S.; Berman, E.; et al. The sloan digital sky survey: Technical summary. *Astron. J.* **2000**, *120*, 1579–1587. [CrossRef]
10. Pourbaix, D.; Knapp, G.R.; Szkody, P.; Ivezić, Ž.; Kleinman, S.J.; Long, D.; Snedden, A.; Nitta, A.; Harvanek, M.; Krzesinski, J.; et al. Candidate spectroscopic binaries in the Sloan Digital Sky Survey. *Astron. Astrophys.* **2005**, *444*, 643–649. [CrossRef]
11. Bellm, E.C.; Kulkarni, S.R.; Graham, M.J.; Dekany, R.; Smith, R.M.; Riddle, R.; Masci, F.J.; Helou, G.; Prince, T.A.; Adams, S.M.; et al. The Zwicky Transient Facility: System Overview, Performance, and First Results. *Publ. Astron. Soc. Pac.* **2019**, *131*, 018002. [CrossRef]

12. Chen, X.D.; Wang, S.; Deng, L.C.; de Grijs, R.; Yang, M.; Tian, H. The Zwicky Transient Facility Catalog of Periodic Variable Stars. *Astrophys. J. Suppl. Ser.* **2020**, *249*, 18. [CrossRef]
13. Cui, X.Q.; Zhao, Y.H.; Chu, Y.Q.; Li, G.P.; Li, Q.; Zhang, L.P.; Su, H.J.; Yao, Z.Q.; Wang, Y.N.; Xing, X.Z.; et al. The Large Sky Area Multi-Object Fiber Spectroscopic Telescope (LAMOST). *Res. Astron. Astrophys.* **2012**, *12*, 1197–1242. [CrossRef]
14. Zhao, G.; Zhao, Y.H.; Chu, Y.Q.; Jing, Y.P.; Deng, L.C. LAMOST spectral survey-An overview. *Res. Astron. Astrophys.* **2012**, *12*, 723–734. [CrossRef]
15. Qian, S.B.; Zhang, J.; He, J.J.; Zhu, L.Y.; Zhao, E.G.; Shi, X.D.; Zhou, X.; Han, Z.T. Physical Properties and Evolutionary States of EA-type Eclipsing Binaries Observed by LAMOST. *Astrophys. J. Suppl. Ser.* **2018**, *235*, 5. [CrossRef]
16. Stoughton, C.; Lupton, R.H.; Bernardi, M.; Blanton, M.R.; Burles, S.; Castander, F.J.; Connolly, A.J.; Eisenstein, D.J.; Frieman, J.A.; Hennessy, G.S.; et al. Sloan Digital Sky Survey: Early Data Release. *Astron. J.* **2002**, *123*, 485–548. [CrossRef]
17. Abazajian, K.; Adelman-McCarthy, J.L.; Agüeros, M.A.; Allam, S.S.; Anderson, S.F.; Annis, J.; Bahcall, N.A.; Baldry, I.K.; Bastian, S.; Berlind, A.; et al. The First Data Release of the Sloan Digital Sky Survey. *Astron. J.* **2003**, *126*, 2081–2086. [CrossRef]
18. Liu, C.; Fu, J.N.; Shi, J.R.; Wu, H.; Han, Z.W.; Chen, L.; Dong, S.B.; Zhao, Y.H.; Chen, J.J.; Zhang, H.T.; et al. LAMOST Medium-Resolution Spectroscopic Survey (LAMOST-MRS): Scientific goals and survey plan. *arXiv* **2020**, arXiv:2005.07210v1.
19. Wu, Y.; Du, B.; Luo, A.L.; Zhao, Y.H.; Yuan, H.L. Automatic stellar spectral parameterization pipeline for LAMOST survey. *IAU Symp.* **2014**, *306*, 340–342. [CrossRef]
20. Luo, A.L.; Zhao, Y.H.; Zhao, G.; Deng, L.C.; Liu, X.W.; Jing, Y.P.; Wang, G.; Zhang, H.T.; Shi, J.R.; Cui, X.Q.; et al. The first data release (DR1) of the LAMOST regular survey. *Res. Astron. Astrophys.* **2015**, *15*, 1095–1124. [CrossRef]
21. Chen, Y.H.; Li, G.W.; Shu, H. The Preliminary Statistical Analysis of LAMOST DR8 Low Resolution AFGK Stars. *Res. Astron. Astrophys.* **2022**, *22*, 055008. [CrossRef]
22. Cenarro, A.J.; Cardiel, N.; Gorgas, J.; Peletier, R.F.; Vazdekis, A.; Prada, F. Empirical calibration of the near-infrared Ca II triplet-I. The stellar library and index definition. *Mon. Not. R. Astron. Soc.* **2001**, *326*, 959–980. [CrossRef]
23. Xiang, M.S.; Liu, X.W.; Yuan, H.B.; Huo, Z.Y.; Huang, Y.; Zheng, Y.; Zhang, H.W.; Chen, B.Q.; Zhang, H.H.; Sun, N.C.; et al. Relative flux calibration for the LAMOST Spectroscopic Survey of the Galactic anticentre. *Mon. Not. R. Astron. Soc.* **2015**, *448*, 90–103. [CrossRef]
24. Bai, Z.R.; Zhang, H.T.; Yuan, H.L.; Li, G.W.; Chen, J.J.; Lei, Y.J.; Yang, H.Q.; Dong, Y.Q.; Wang, G.; Zhao, Y.H. Sky subtraction for LAMOST. *Res. Astron. Astrophys.* **2017**, *17*, 91. [CrossRef]
25. Chen, Y.H.; Duan, C.M.; Shu, H. Multi-band Photometric and Spectroscopic Analysis of the Dwarf Nova IU Leo. *Res. Astron. Astrophys.* **2026**, *26*, 015001. [CrossRef]
26. Herbig, G.H. The Diffuse Interstellar Bands. *Astron. Astrophys.* **1995**, *33*, 19–74. [CrossRef]
27. Keller, S.C.; Schmidt, B.P.; Bessell, M.S.; Conroy, P.G.; Francis, P.; Granlund, A.; Kowald, E.; Oates, A.P.; Martin-Jones, T.; Preston, T.; et al. The SkyMapper Telescope and Southern Sky Survey. *Publ. Astron. Soc. Aust.* **2007**, *24*, 1–12. [CrossRef]
28. Skrutskie, M.F.; Cutri, R.M.; Stiening, R.; Weinberg, M.D.; Schneider, S.; Carpenter, J.M.; Beichman, C.; Capps, R.; Chester, T.; Elias, J.; et al. The Two Micron All Sky Survey (2MASS). *Astron. J.* **2006**, *131*, 1163–1183. [CrossRef]
29. Wright, E.L.; Eisenhardt, P.R.M.; Mainzer, A.K.; Ressler, M.E.; Cutri, R.M.; Jarrett, J.; Kirkpatrick, J.D.; Padgett, D.; McMillan, R.S.; Skrutskie, M.; et al. The Wide-Field Infrared Survey Explore (WISE): Mission Description and Initial on-orbit Performance. *Astron. J.* **2010**, *140*, 1868–1881. [CrossRef]
30. Covey, K.R.; Ivezić, Ž.; Schlegel, D.; Finkbeiner, D.; Padmanabhan, N.; Lupton, R.H.; Agüeros, M.; Bochanski, J.J.; Hawley, S.L.; West, A.A.; et al. Stellar SEDs from 0.3 to 2.5 μm: Tracing the Stellar Locus and Searching for Color Outliers in the SDSS and 2MASS. *Astron. J.* **2007**, *134*, 2398–2417. [CrossRef]
31. Lindegren, L.; Klioner, A.; Hernández, J.; Bombrun, A.; Ramos-Lerate, M.; Steidelmüller, H.; Bastian, U.; Biermann, M.; de Torres, A.; Gerlach, E.; et al. Gaia Early Data Release 3 The Astrometric solution. *Astron. Astrophys.* **2021**, *649*, A2. [CrossRef]
32. Krolikowski, D.M.; Kraus, A.L.; Rizzuto, A.C. Gaia EDR3 Reveals the Substructure and Complicated Star Formation History of the Greater Taurus-Auriga Star-forming Complex. *Astron. J.* **2021**, *162*, 110. [CrossRef]
33. Hou, W.; Luo, A.L.; Dong, Y.Q.; Chen, X.L.; Bai, Z.R. Spectroscopically Identified Cataclysmic Variables from the LAMOST Survey. II. Period Estimates. *Astron. J.* **2023**, *165*, 148. [CrossRef]
34. Borucki, W.J.; Koch, D.; Basri, G.; Batalha, N.; Brown, T.; Caldwell, D.; Caldwell, J.; Christensen-Dalsgaard, J.; Cochran, W.D.; DeVore, E.; et al. Kepler Planet-Detection Mission: Introduction and First Results. *Science* **2010**, *327*, 977–980. [CrossRef]
35. Ricker, G.R.; Winn, J.N.; Vanderspek, R.; Latham, D.W.; Bakos, G.Á.; Bean, J.L.; Berta-Thompson, Z.L.; Brown, T.M.; Buchhave, L.; Butler, N.R.; et al. Transiting Exoplanet Survey Satellite (TESS). *Proc. SPIE* **2014**, *9143*, 20.
36. Dekany, R.; Smith, R.M.; Riddle, R.; Feeney, M.; Porter, M.; Hale, D.; Zolkower, J.; Belicki, J.; Kaye, S.; Henning, J.; et al. The Zwicky Transient Facility: Observing System. *Publ. Astron. Soc. Pac.* **2020**, *132*, 038001. [CrossRef]
37. Masci, F.J.; Laher, R.R.; Rusholme, B.; Shupe, D.L.; Groom, S.; Surace, J.; Jackson, E.; Monkewitz, S.; Beck, R.; Flynn, D.; et al. The Zwicky Transient Facility: Data Processing, Products, and Archive. *Publ. Astron. Soc. Pac.* **2019**, *131*, 018003. [CrossRef]

38. Richmond, A.; White, N. HEASARC. The Design an Architecture of an Astrophysics Information System. *Bull. Astron. Soc.* **1994**, *26*, 995–998.
39. Davenport, J.R.A. The Kepler Catalog of Stellar Flares. *Astron. J.* **2016**, *829*, 23. [CrossRef]
40. Günther, M.N.; Zhan, Z.C.; Seager, S.; Rimmer, P.B.; Ranjan, S.; Stassun, K.G.; Oelkers, R.J.; Daylan, T.; Newton, E.; Kristiansen, M.H.; et al. Stellar Flares from the First TESS Data Release: Exploring a New Sample of M Dwarfs. *Astron. J.* **2020**, *159*, 60. [CrossRef]
41. Howard, W.S.; MacGregor, M.A. No Such Thing as a Simple Flare: Substructure and Quasi-periodic Pulsations Observed in a Statistical Sample of 20 s Cadence TESS Flares. *Astron. J.* **2022**, *926*, 204. [CrossRef]
42. Coughlin, M.W.; Burdge, K.; Duev, D.A.; Katz, M.L.; van Roestel, J.; Drake, A.; Graham, M.J.; Hillenbrand, L.; Mahabal, A.A.; Masci, F.J.; et al. The ZTF Source Classification Project-II. Periodicity and variability processing metrics. *Mon. Not. R. Astron. Soc.* **2021**, *505*, 2954–2965. [CrossRef]
43. Jia, Q.; Chen, X.D.; Wang, S.; Deng, L.C.; Luo, Y.P.; Jiang, Q.Q. Multimode δ Sct stars from the Zwicky Transient Facility Survey. *Astrophys. J. Suppl. Ser.* **2024**, *273*, 7. [CrossRef]
44. Chen, X.H.; Li, Y.; Lin, G.F.; Chen, Y.H.; Guo, J.J. Exploring the helium core of the δ Scuti star COROT 102749568 with asteroseismology. *Astron. J.* **2017**, *834*, 146. [CrossRef]

Disclaimer/Publisher's Note: The statements, opinions and data contained in all publications are solely those of the individual author(s) and contributor(s) and not of MDPI and/or the editor(s). MDPI and/or the editor(s) disclaim responsibility for any injury to people or property resulting from any ideas, methods, instructions or products referred to in the content.